REMOTE ESTIMATION OF A MANAGED PINE FOREST EVAPOTRANSPIRATION WITH GEOSPATIAL TECHNOLOGY

S. Panda, D. M. Amatya, G. Sun, A. Bowman

ABSTRACT. *Remote sensing has increasingly been used to estimate evapotranspiration (ET) and its supporting parameters in a rapid, accurate, and cost-effective manner. The goal of this study was to develop remote sensing-based models for estimating ET and the biophysical parameters canopy conductance (g_c), upper-canopy temperature, and soil moisture for a mature loblolly pine forest (*Pinus taeda* L.) in the Parker Tract in eastern North Carolina. To validate the remote sensing approach, we acquired long-term on-site eddy flux measurements, including micrometeorological variables and water and energy fluxes. Other measured and derived ET-associated parameters include forest g_c, leaf area index, canopy absorbed radiation, canopy temperature, and soil moisture. Multi-temporal cloud-free (≤10% cloud cover) Landsat 7 ETM+ satellite images from 2006-2012 were acquired. Field data for the 2 h (12:00 noon to 2:00 p.m.) means were used in the model, coinciding with the image acquisition time. Individual Landsat bands (1 through 7) and developed image vegetation indices (NDVI, SAVI, and VVI) for the study site were obtained through automated geospatial models and were correlated to measured ET flux and related parameters. An excellent coefficient of determination (R^2 = 0.93, n = 42) was obtained for the upper-canopy temperature versus band 6 (thermal infrared) model. However, a low correlation (R^2 = 0.36, n = 6) was obtained for g_c versus band 5 (mid-infrared) model. The correlation for soil moisture versus band 7 was poor (R^2 = 0.05, n = 42), perhaps due to heavy canopy and pine litter ground cover. However, the ET estimation model with multiple image information variables, such as bands 5 and 7, provided a good correlation (R^2 = 0.55, n = 35) with less spatial and temporal variation in the datasets, along with no data mining application in model building. Therefore, this study suggests that the remote sensing approach is promising for estimating ET with good accuracy (average model prediction residual error = 25.46 W m^{-2}, 6.18% of the average ET values used in the analysis) for a mature homogenous pine forest. Further work is needed to develop robust remote sensing-based ET models by including spatial variability, sound data mining, high-resolution imagery, and advanced image processing to account for potential modeling uncertainties.*

Keywords. *Canopy conductance, Canopy temperature, Evapotranspiration, Model builder, NDVI, Python script, SAVI, Soil moisture, Spatial analysis, VVI.*

Plant and soil/understory litter evaporation and transpiration (or evapotranspiration, ET) is a major component of the hydrological cycle. Accurate estimation of ET and its spatial and temporal distribution is of key importance for hydrological and meteorological applications, including regional-scale water balance (Sun et al., 2011). Evapotranspiration has direct impacts on hydrology, crop growth, and biomass production. Forest cover alteration, including intercropping to accommodate bioenergy crops such as switchgrass, may change the ET and water balance of forest ecosystems. The ET rate of an ecosystem depends on soil moisture and vegetation factors as well as climatic variables such as air and canopy temperature, radiation, vapor pressure, wind speed, and characteristics of the evaporating surface (Viesmann and Lewis, 2004). Plant evaporation occurs mostly from above-canopy interception as a function of canopy storage capacity and density (Amatya et al., 1996), and understory litter transpiration occurs by uptake and transport of water from the soil/aquifer system by plant roots, branches, and stems, eventually diffusing from plant leaves into the atmosphere (Senay et al., 2013). The atmospheric boundary layer conditions at the plant canopy surface, driven by solar energy (radiation and air temperature), wind, and humidity, and their capacity to transport vapor away from the evaporative surface are the guiding factors for ET (Viesmann and Lewis, 2004).

Leaf area index (LAI), canopy temperature (T_c), canopy (g_c) or leaf stomatal (g_s) conductance (hereafter referred to as stomatal conductance), wind velocity, and soil moisture

Submitted for review in January 2015 as manuscript number NRES 11134; approved for publication by the Natural Resources & Environmental Systems Community of ASABE in August 2016 as part of the Special Collection on Evapotranspiration: Monitoring & Modeling in Multiple Land Uses, published in issue 2.

Mention of company or trade names is for description only and does not imply endorsement by the USDA. The USDA is an equal opportunity provider and employer.

The authors are **Sudhanshu Panda,** Professor, Institute of Environmental Spatial Analysis, University of North Georgia, Oakwood, Georgia; **Devendra M. Amatya, ASABE Member,** Research Hydrologist, Center for Forested Wetlands Research, USDA Forest Service, Cordesville, South Carolina; **Ge Sun,** Research Hydrologist, Eastern Forest Environmental Threat Assessment Center, USDA Forest Service, Raleigh, North Carolina; **Adam Bowman,** Student, Institute of Environmental Spatial Analysis, University of North Georgia, Oakwood, Georgia. **Corresponding author:** Sudhanshu Panda, Institute of Environmental Spatial Analysis, 3820 Mundy Mill Road, Oakwood, GA 30566; phone: 678-717-3594; e-mail: Sudhanshu.Panda@ung.edu.

or volumetric water content are the most important parameters for ET estimation (Panda et al., 2014). LAI is defined as the single-sided surface area of leaves per unit area of soil ($m^2 m^{-2}$) and is a key parameter in a variety of forest ecosystem processes, including interception of light and rain, transpiration, photosynthesis, and soil heterotrophic respiration (le Maire et al., 2006). LAI is a seasonal parameter and is an indicator of crop growth; thus, ET and LAI correlate very well (Sun et al., 2011). LAI was also one of the hydrologic parameters that was recently discussed in parameterization guidelines and considerations for hydrologic models by Malone et al. (2014). Indirect optical methods (e.g., LAI-2200 Plant Canopy Analyzer, LI-COR, Lincoln, Neb.) or hemispherical photographs and semi-direct methods using litter collection and allometry are used for local estimation of LAI (Malone et al., 2014; Brauman et al., 2012; Sampson et al., 2011; le Maire et al., 2006). However, these methods are time consuming, cumbersome, and costly. Efficient use of remotely sensed data to estimate LAI is prevalent, as empirical relationships between LAI and spectral vegetation indices (SVI) such as the normalized difference vegetation index (NDVI) are widely used in the remote sensing community (Rao et al., 2006; Chen et al., 1997; Turner et al., 1999). LAI is a valuable driver in the scaling effort, as it is well correlated with NDVI derived from remote sensing images (Hwang et al., 2009). However, NDVI-based LAI estimation has several known shortcomings (Qi et al., 2000). Anderson et al. (2004) and Wang et al. (2005) found discrepancies in estimating LAI values >3.5 $m^2 m^{-2}$ with NDVI. Wang et al. (2005) and Soudani et al. (2006) suggested that the relationship established between LAI and NDVI for a particular satellite sensor may not be applicable to other sensors or to describe temporal variations using measurements from the same sensor. Qi et al. (2000) and Colombo et al. (2003) showed that the relationship of LAI and vegetation index could be specific to a vegetation species and study site. Nevertheless, estimation of LAI for a homogenous pine forest using remotely sensed image based vegetation indices could be useful.

According to Hilker et al. (2013), transpiration is directly linked to stomatal conductance (g_s). Local measurement of stomatal conductance is performed with an indirect optical method (Brauman et al., 2012) or with a semi-direct method using a vapor pressure deficit algorithm (Pearcy et al., 1989; Sack and Scoffoni, 2012), but these methods are costly and time consuming. Stomatal conductance of pine needles has been measured and used for estimating and modeling transpiration of pine forests (McCarthy et al., 1991; Amatya et al., 1996; Amatya and Skaggs, 2001). Hilker et al. (2013) suggested that satellite-based determination of photosynthesis or gross primary production (GPP) could be used to quantify transpiration rates through g_s (Panda et al., 2014). Canopy conductance (g_c) is generally approximated as a product of g_s and LAI (Jensen et al., 1990; Amatya and Skaggs, 2001; Amatya et al., 1996; Nghi et al., 2008; Brauman et al., 2012; Tian et al., 2012; Amatya et al., 2014), although the maximum g_s may also be estimated as a function of measured ET, vapor pressure deficit, and other environmental variables (Morris et al., 1998), as will be shown below.

Canopy temperature can serve as a surrogate for the amount of evaporation and transpiration through the plant canopy and can be estimated with direct measurement using thermometers (Bastiaanssen et al., 1998). However, routine *in situ* measurement of this plant parameter is time consuming and expensive (Sampson et al., 2011; Panda et al., 2014). The thermal band of Landsat satellite imagery is used for estimation of canopy temperature (Lee, 1994; Senay et al., 2013; Panda at el., 2014). Satellite imagery approaches are generally based on principles of the surface energy balance, using the remotely derived land surface temperature as a proxy indicator of surface water status (Cammalleri et al., 2013). A review by Wang and Qu (2009) showed that numerous studies have been conducted on remote estimation of soil volumetric water content using satellite, aerial, or simple digital photographic image analysis. Recent studies show that remotely sensed data, especially freely available 30 m spatial resolution, 16-day temporal resolution Landsat Thematic Mapper (TM) images, can be used to efficiently estimate g_s, canopy temperature, LAI, and ET of forest vegetation (Rouse et al., 1973; Curran, 1980; Moran et al., 1994; Carter, 1998; Justice et al., 1998; Olioso et al., 1999; North, 2002; Provoost et al., 2005; le Maire et al., 2006; Panda et al., 2011; Nouri et al., 2013; Hafeez et al., 2002; Senay et al., 2013; Panda et al., 2014).

Vegetation indices (e.g., NDVI or soil-adjusted vegetation index [SAVI]) developed with near-infrared (NIR) and red wavebands can be used to remotely determine many forest hydrologic parameters, including LAI (Lillesand and Kiefer, 1994; Gamon et al., 1995; Narasimhan et al., 2003; Rao et al., 2006; Senay et al., 2013). Remote estimation of LAI is typically conducted using selected individual-band spectral reflectance or digital number (DN) values or a combination of values with the development of spectral indices such as NDVI or SAVI (Panda et al., 2014). Remote measurement of g_s is conducted using a suitable band (typically, mid-infrared, MIR) of Landsat satellite imagery (Lee, 1994; Carter, 1998; Panda et al., 2014).

The goal of this study was to develop geospatial models to estimate eco-hydrologic parameters that can ultimately determine the ET and growth of a managed pine forest using remotely sensed imagery. The specific objectives of the study were to:

1. Develop geospatial models to estimate three ET parameters, i.e., plant canopy conductance (g_c), above-canopy temperature (T_c), and soil moisture (SM), using freely available Landsat 7 ETM+ imagery.
2. Develop geospatial models to estimate latent heat flux (converted to ET) using freely available Landsat 7 ETM+ imagery.
3. Establish empirical algorithms based on the image information to predict ET and ET parameters remotely.

METHODOLOGY

STUDY SITE

The study site (fig. 1) was located in Weyerhaeuser's Parker Tract (TPT) pine plantation in the lower Coastal Plain region of North Carolina near Plymouth. The study site was

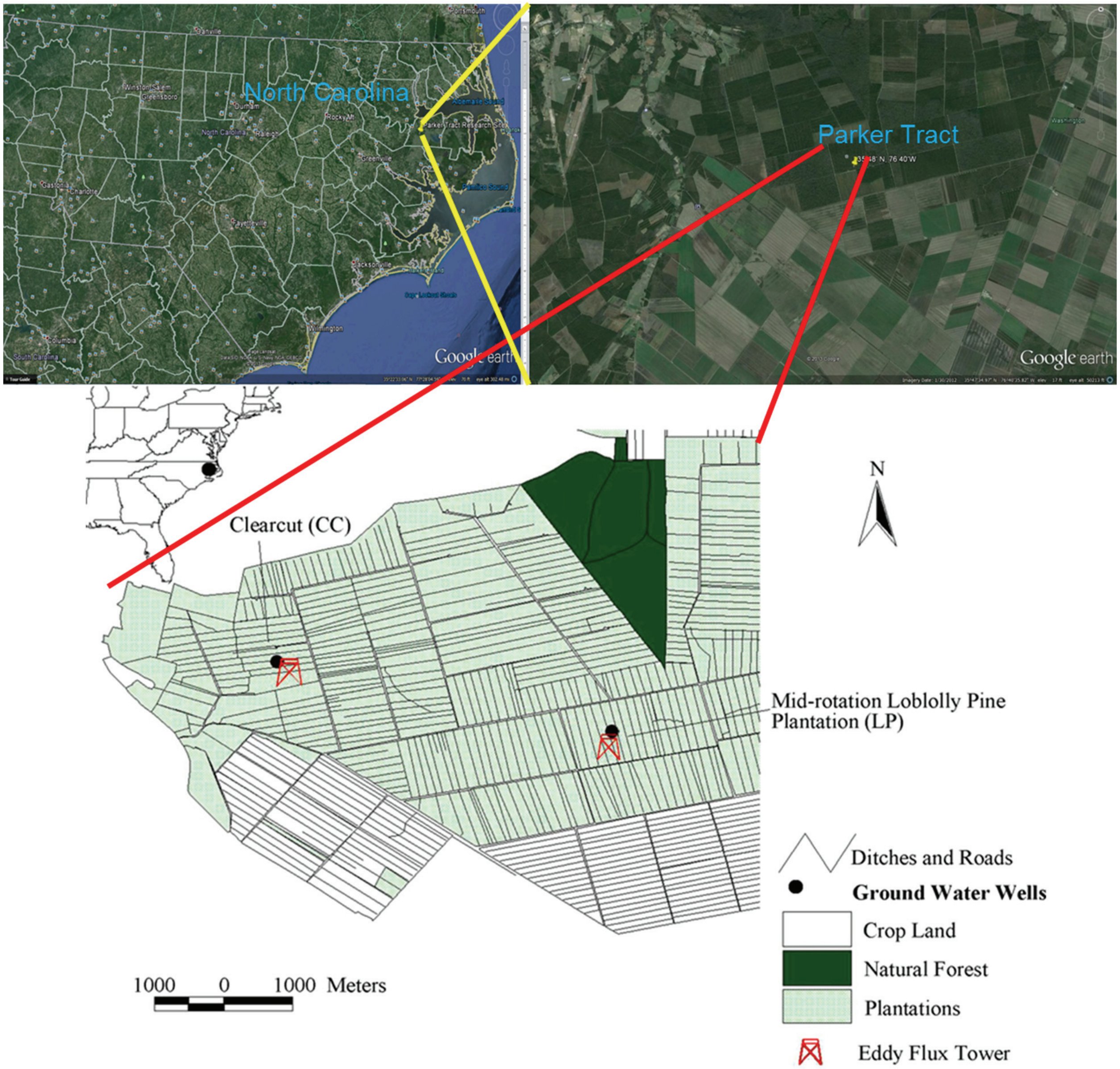

Figure 1. Study area location and instrumentation for climatologic data acquisition and plant growth monitoring.

managed by the USDA Forest Service Southern Research Station, Eastern Forest Environmental Threat Assessment Center (EFETAC) (USDA Forest Service, 2014). Ongoing studies are being conducted of two different forest management practices based on land use: (1) North Carolina Loblolly Pine (NCLP) (35° 48′ N, 76° 40′ W) at ~5 m elevation above mean sea level (amsl) and (2) North Carolina Clear-Cut (NCCC) (35° 48′ N, 76° 42′ W) at ~6 m elevation amsl and about 4 km from the NCLP site (USDA Forest Service, 2014). This study was conducted on the loblolly pine (*Pinus taeda* L.) land cover with various stand ages and native hardwoods forests. The topography of the study area is flat, with a ground elevation less than 8 m amsl, and drained with ditches approximately 90 to 100 m apart (Sun et al., 2010). The area has poorly drained soils with predominant soil types classified as loamy, mixed, dysic, thermic Terric Haplosaprists in the Cape Fear and Belhaven series (USDA Forest Service, 2014). The long-term (1945 to 2008) average annual precipitation at the site was 1320 mm ±211 mm and was evenly distributed, with a mean annual temperature of 15.5°C (Sun et al., 2010). The annual growing season of pine averaged about 195 days (Sun et al., 2010). The research site was well instrumented for climatologic data acquisition and plant growth monitoring, with an eddy flux tower (fig. 2) located in the middle of the 90 ha, mid-rotation loblolly pine stand established in 1992 after clear-cutting the previous mature pine plantation (Sun et al., 2010).

Data Acquisition

The eddy covariance method for climatologic and hydrologic data measurements, including simultaneous measurement of vertical wind speed and water vapor density (and thus vertical moisture flux or ET), related parameters of LAI, soil moisture, canopy temperature, and CO_2 fluxes, and the derived estimation of g_s, has gained popularity in recent years due to high temporal-scale data acquisition, perfor-

Figure 2. Eddy flux tower at the research site used to monitor climatologic data and plant growth.

mance improvements, and reduced costs of fast-response monitoring sensors (Wilson et al., 2001; Shuttleworth, 2008; Sun et al., 2010). The eddy flux tower (fig. 2) at the study site has been collecting climatologic data continuously since 2006.

The open-path eddy covariance system consists of an infrared gas analyzer (LI-7500, LI-COR, Lincoln, Neb.) to measure carbon dioxide and water vapor densities, a three-dimensional sonic anemometer (CSAT3, Campbell Scientific, Logan, Utah) to measure directional wind velocity, and a data logger (CR5000, Campbell Scientific) (Sun et al., 2010). Micrometeorological variables measured at the tower included above-canopy air temperature (HMP45AC, Vaisala, Inc., Louisville, Colo.), photosynthetically active radiation (PAR) (LI-190, LI-COR), downward and upward shortwave and longwave radiation (CNR-1, Kipp and Zonen, Delft, Netherlands). The top 30 cm averaged volumetric soil moisture content was measured continuously using a vertically inserted time domain reflectometer (CS616, Campbell Scientific). Beginning on 10 May 2007, the soil moisture profile at 10, 20, 30, 40, 50, 60, 80, and 120 cm depths was measured using EnviroSCAN sensors (Sentek Sensor Technologies, Stepney, Australia) at a separate location at the NCLP site. ET data were collected as vertical latent energy flux at the tower along with various other climatologic parameters (Sun et al., 2010), which were not part of our analysis in this study. Daily maximum canopy conductance ($g_{c,\max}$) was calculated using the Morris et al. (1998) equation (eq. 1), as suggested by Noormets et al. (2010), with parameters estimated from eddy flux tower data:

$$g_{c.\max} = \frac{pER_w}{\rho \mathrm{VPD} R_d} \quad (1)$$

where g_c is canopy conductance (m s^{-1}), p is atmospheric pressure (kPa), E is evapotranspiration (kg m^{-2} s^{-1}), ρ is air density (kg m^{-3}), VPD is vapor pressure deficit (kPa), and R_d and R_w are universal gas constants for dry air and water vapor, respectively, where R_w/R_d = 1.609. We used the half-hourly values of evapotranspiration and vapor pressure deficit from the eddy flux data for the 12:00 noon to 2:00 p.m. time period, consistent with the satellite image-collection passes, to calculate $g_{c,\max}$ and then used this value to compare with g_s from the satellite images. The daily $g_{c,\max}$ is the maximum g_c generally observed when the canopy-level vapor pressure deficit is within 1 to 1.5 kPa (Oren et al., 1999; Ambrose et al., 2010).

Cloud-free (≤10% cloud cover) Landsat ETM+ 7-band satellite images were acquired for 2006 and 2012 from the U.S. Geological Survey (USGS) Map Viewer site (http://viewer.nationalmap.gov/viewer/). A total of 56 Landsat ETM+ images were acquired. Corresponding field data (ET, canopy temperature, and soil moisture) were available for the acquired image dates, as the data that were collected continuously at the tower at 30 min intervals were available for our research. However, for each image date, correct hydrologic parameter data were not available due to instrument malfunction. The $g_{c,\max}$ data could be calculated only for 2012 using equation 1, as the parameters required in equation 1 were not available for other years. As a result, only six datasets were used in the $g_{c,\max}$ model development. A total of 42 data sets were available for development of canopy temperature and soil moisture models. Only 35 correct data sets were available for ET model development.

Spectral information is particularly useful in applications that involve mapping and modeling of the biophysical properties of objects, such as water quality, plant vigor, soil nutrients, etc., because Landsat individual bands support very specific Earth observation applications (Panda et al., 2015). Figure 3 shows how Landsat individual bands, or combinations of bands through ratio development, can be used to estimate the eco-hydrologic parameters of interest in this study. According to Panda et al. (2015), satellite wavebands were specifically designed and are useful (as supported by numerous studies) for remote estimation of ecological features on Earth (fig. 3).

We developed an input (image information) and output (ecohydrologic parameter) correlation relationship chart for each model (table 1). Based on figure 3, the field-measured volumetric water content or soil moisture was correlated with band 7 (MIR) means, derived $g_{c,\max}$ was correlated with band 5 (MIR) means, and canopy temperature was correlated with band 6 (thermal infrared [TIR]) means of the Landsat ETM+ images for model development. As discussed above, NDVI alone may not efficiently estimate LAI and ET remotely. Therefore, SAVI, NDVI, a newly developed vegetation vigor index (VVI), and mean values of bands 5, 6, and 7 were used in the ET estimation model development.

Multicollinearity analysis was completed to determine the correlation among the predictors, and a threshold of 40% was used to determine if a strong internal correlation existed among the predictors. In addition, stepwise regression analyses were completed with datasets, both with and without outlier deletion, to determine the best predictor-based models for estimating ET. Finally, individual models were created using different combinations of predictors. The combination with the best model results was chosen for the remote sensing based ET estimation algorithm.

Vegetation indices were developed using equation 2 for NDVI, equation 3 for SAVI, and equation 4 for VVI:

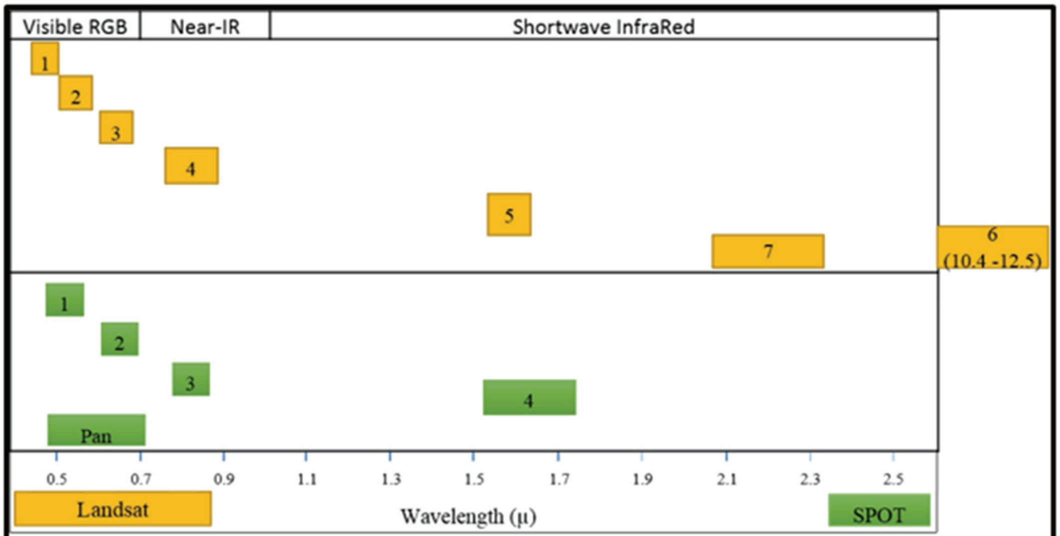

Landsat 7 ETM+ Band (μm)	Applications	SPOT 4 Band (μm)
Band 1 – Blue IR (0.45 – 0.52)	Coastal water mapping, soil/vegetation differentiation, deciduous/coniferous differentiation	
Band 2 – Green (0.52 – 0.60)	Green reflectance from healthy vegetation, iron content in rocks and soil	Band 1 (0.50 – 0.59) (Green)
Band 3 – Red (0.63 – 0.69)	Chlorophyll absorption for plant differentiation	Band 2 (0.61 – 0.68) (Red)
Band 4 – Near IR (0.76 – 0.90)	Biomass survey, water body delineation	Band 3 (0.79 – 0.89) (Near-Infrared)
Band 5 – Mid IR (1.55 – 1.75)	Plant moisture content, cloud/snow differentiation	Band 4 (1.58 – 1.75) (Mid-Infrared)
Band 6 – Thermal IR (10.4 – 12.5)	Thermal mapping, soil moisture	
Band 7 – Mid IR (2.08 – 2.35)	Soil analysis	

ETM = Enhanced Thematic Mapper; IR = Infrared; Mid IR (MIR) = Middle Infrared

Figure 3. General comparison of Landsat and SPOT spectral bands for Earth observation applications (adapted from Panda et al., 2015).

Table 1. Input-output correlation relationship chart for model development.

Ecohydrologic Parameter	Image Information	
Evapotranspiration	SAVI means, NDVI means, VVI means, and individual band 5, 6, and 7 DN means	Mean calculated ET from eddy flux tower data (12:00 h to 2:00 h) (W m^{-2})
Soil moisture	Band 7 means	Mean 0-30 cm depth time domain reflectometry data (%)
Canopy temperature	Band 6 means	Mean instrument data (12:00 h to 2:00 h) (°C)
Canopy conductance	Band 5 means	Mean calculated from equation 1 (12:00 h to 2:00 h) (m s^{-1})

$$\mathrm{NDVI} = \frac{(\rho_{ir} - \rho_r)}{(\rho_{ir} + \rho_r)} \quad (2)$$

$$\mathrm{SAVI} = \left[\frac{(\rho_{ir} - \rho_r)}{(\rho_{ir} + \rho_r + L)}\right] \times (1 + L) \quad (3)$$

$$\mathrm{VVI} = \frac{(\rho_{ir} - \rho_g)}{(\rho_{ir} + \rho_g)} \quad (4)$$

where ρ_r, ρ_g, and ρ_{ir} are spectral reflectance from the red, green, and NIR band images, respectively, and L is a constant that represents the vegetation density. Huete (1988) defined optimal adjustment factors of L = 0.25 for high vegetation density in the field, L = 0.5 for intermediate vegetation density, and L = 1 for low vegetation density.

Image Analysis

Image Information Development

We used a 10 pixel × 10 pixel window surrounding the eddy flux tower, which covered an area of 300 m × 300 m (90,000 m^2). The pixels of the 10 pixel × 10 pixel window of the Landsat 7 ETM+ images were between two scan lines for all the images used in this study. Therefore, non-existence of digital data in the scan lines did not interfere with the image analysis. Figure 4 shows examples of bands 2, 3, 4, 5, 6, and 7 from a single-date Landsat image used in our index development and subsequent model development.

Individual bands (green, red, and NIR) were used to develop the NDVI, SAVI, and VVI indices in ArcGIS 10.1 with the Raster Calculator tool using equations 2, 3, and 4, respectively. For SAVI raster development, an L factor of 0.85 was used to represent the dense, homogenous, mature pine plantation.

Image Analysis Automation

Automated geospatial models were used for plot size (10×10 pixels) image extraction. The automation of the image analysis helped in processing a total of 448 images in a rapid and efficient way. Python scripts were written for vegetation index (NDVI, SAVI, and VVI) image development. Figure 5 shows an example of a Python script (for VVI development) that runs on the ArcGIS 10.1 platform for efficient batch processing. This automation in image analysis saved time. The Python script was written for extracting means of digital images by averaging all 100 pixel values.

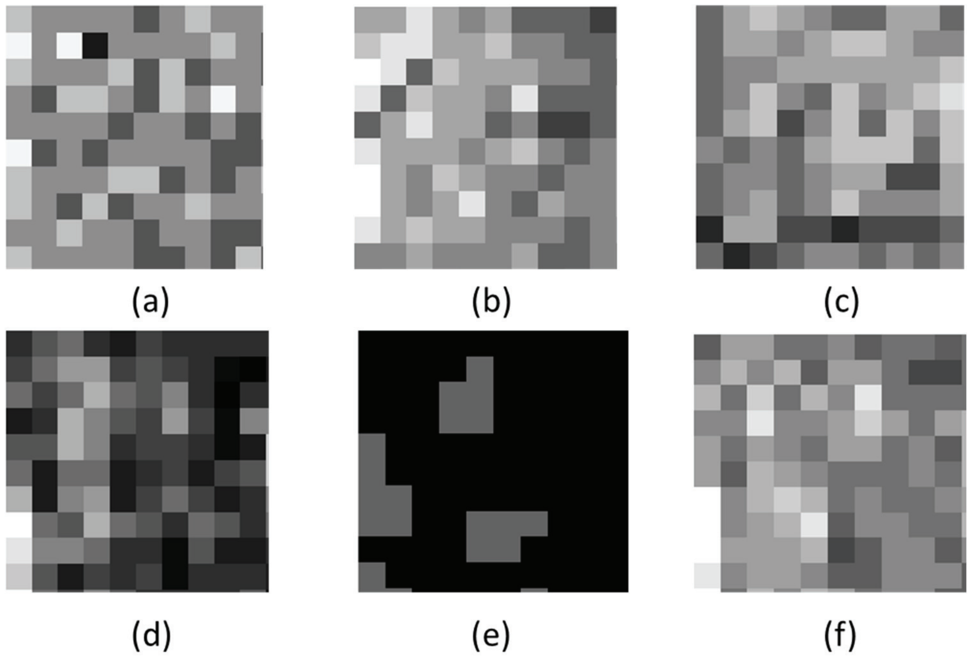

Figure 4. Examples of individual Landsat images of the study area (300 m × 300 m) for (a) band 2, green, (b) band 3, red, (c) band 4, NIR, (d) band 5, MIR, (e) band 6, TIR, and (f) band 7, MIR.

```
import os, glob

a = []
for file in glob.glob('*.TIF'):
    a.append(file)


count = 0
count2 = 1
for item in a:

    #Check out the Spatial Analyst extension (must be available to check out
    arcpy.CheckOutExtension("spatial")

    #Add your workspace here
    env.workspace = r"C:/Users/Adam's/Desktop/cvi"

    #Create raster directory and specify inputs. It references the input
    result = "{}".format(a[count][0:8] + 'cvi.tif')
    ShortIR = a[count2]
    Green = a[count]

    #Create Numerator and Denominator rasters as variables and cvi output
    Num = arcpy.sa.Raster(ShortIR) - Raster(Green)
    Denom = arcpy.sa.Raster(ShortIR) + Raster(Green)
    ShortIR_eq = arcpy.sa.Divide(Num, Denom)
    print "Dividing"
    #Saving output to result output you specified above
    ShortIR_eq.save(result)
    print "Successful"
    count+=2
    count2+=2
```

Figure 5. Python script written for VVI raster development on the ArcGIS 10.1 platform.

Results and Discussion

Plant Canopy Temperature Model

Upper-canopy air temperature was correlated by a first-order exponential relationship to the band 6 (TIR) mean with a high coefficient of determination ($R^2 = 0.93$, $n = 42$), suggesting an excellent relationship for mature loblolly pine trees (fig. 6). This is very promising because canopy temperature is a major parameter used to estimate ET of pine forests through remotely sensed image information. TIR bands are a common means of accurately estimating radiated heat energy from any object on the surface of the Earth, and these results provide further confirmation.

Leaf Canopy Conductance Model

Figure 7 represents the correlation model fitted with a first-order polynomial for the band 5 (MIR) means and the corresponding calculated or derived $g_{c,\max}$ values using equation 1. As mentioned previously, only six measurements were available for a single year (2012) to develop this model. The coefficient of determination ($R^2 = 0.36$, $n = 6$) was obtained with these limited field observations for the $g_{c,\max}$ versus band 5 model. This suggests that our study could not establish a relationship between Landsat band 5 (MIR) means and $g_{c,\max}$ for pine trees. This was attributed to the lack of sufficient observations (data) in model development. Further study is essential to determine if a relationship exists between $g_{c,\max}$ versus Landsat band 5 (MIR) or other remotely sensed data.

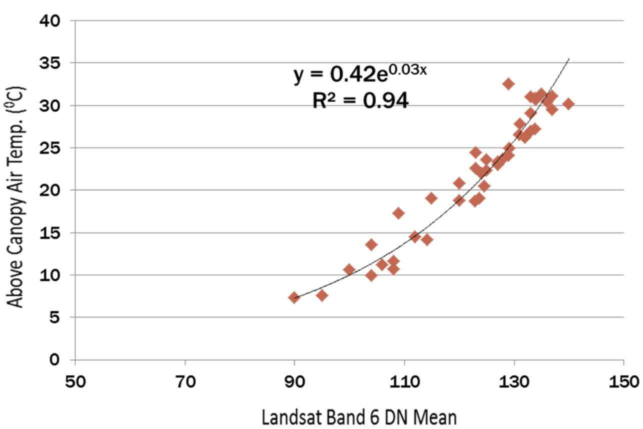

Figure 6. Exponential model developed for upper-canopy air temperature using band 6 (TIR) mean ($n = 42$).

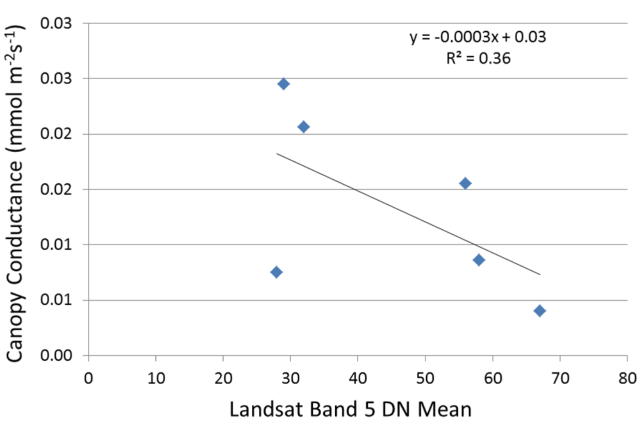

Figure 7. First-order polynomial fitted for canopy conductance versus band 5 (MIR) correlational model ($n = 6$).

Soil Moisture Estimation Model

Figure 8 represents the correlation model fitted with a first-order polynomial for the band 7 (MIR) DN means and the corresponding field-measured soil moisture in the mature pine forest planted in 1992 with an almost closed canopy cover. These managed pine forests reach canopy closure at stand ages of 15 years or more (Amatya et al., 1996; Amatya, 1993). The mature pine stand under observation in this study was 20 years old. Although sufficient field observations ($n = 42$) were used in the soil moisture versus band 7 correlation model development, the resulting R^2 of 0.05 suggests no relationship between Landsat image bandwidth-based values and soil moisture for such a mature pine forest. We conclude that the lack of correlation can be attributed to the fact that the Landsat satellite could not view the ground surface in the mature pine forest with a closed canopy and/or litter covering the forest floor. Future studies may be able to estimate soil moisture using Landsat band 7 means for young pine, where canopy cover is thin and open and between-row bare soil is visible.

Pine ET Remote Estimation Model

Initially, a multi-collinearity analysis was conducted with all six input parameters. The calculated correlation coefficients in the collinearity matrix in table 2 suggest that SAVI (0.96) is strongly correlated with NDVI, and the VVI input parameter is collinear with all other input parameters (threshold is >0.3). A multivariate correlation model using pine ET as a dependent variable and all six [band 5 (MIR), band 6 (TIR), band 7 (MIR), NDVI, SAVI, and VVI] plot raster means as independent input parameters was developed (model 1 in table 3). A total of 35 measurements covering seven years (2006-2012) of the study period were available for the model development. Good correlation ($R^2 = 0.61$) was obtained between the Landsat image data and ET for this

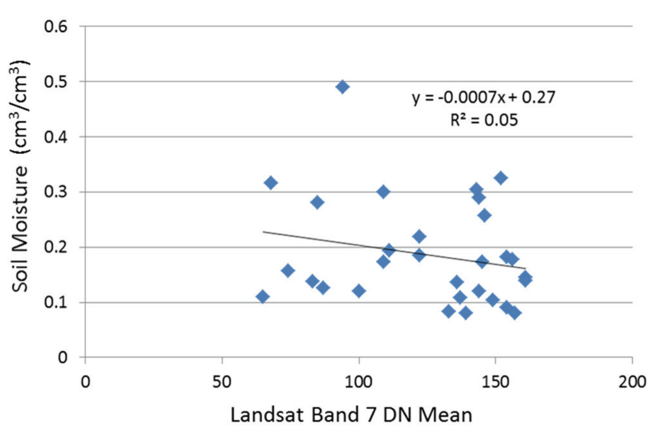

Figure 8. First-order polynomial fitted for the soil moisture of the dense mature pine forest versus band 7 (MIR) correlational model ($n = 42$).

Table 2. Multi-colinearity matrix result of all six input parameters used with the initial model.

	B5	B6	B7	NDVI	SAVI	VVI
B5	1	-	-	-	-	-
B6	0.23	1.00	-	-	-	-
B7	0.29	-0.10	1.00	-	-	-
NDVI	-0.04	0.05	-0.15	1.00	-	-
SAVI	0.04	0.05	-0.11	0.96	1.00	-
CVI	0.30	0.39	-0.34	0.42	0.42	1.00

Table 3. Multiple regression model results for various combination of input parameters to predict hourly ET.

Model	Input Parameter Combination	R^2	Adjusted R^2	Model Prediction Residual Error (W m^{-2})	Standard Error (W m^{-2})
1	B5, B6, B7, NDVI, SAVI, VVI	0.61	0.53	23.78 (6.08%)	157.31
2	B5, B6, B7, NDVI, VVI	0.61	0.54	24.19	155.40
3	B5, B6, B7, NDVI	0.60	0.54	24.60	155.32
4	B5, B6, B7, SAVI	0.59	0.53	24.58	157.10
5	B6, B7, NDVI	0.54	0.51	25.70	161.55
6	B7, NDVI	0.53	0.50	26.25	162.42
7	B6, NDVI	0.12	0.06	35.97	222.58
8	B5, NDVI	0.08	0.02	36.75	277.40
9	B5, B6, B7	0.56	0.52	25.25	158.75
10	B5, B6	0.05	-0.01	56.52	231.13
11	B5, B7	0.55	0.53	25.46	157.54
12	B6, B7	0.52	0.49	26.46	163.69

mature pine forest. For the average ET (n = 35) value of 390.95 W m^{-2}, an average residual error of 23.78 W m^{-2} (6.08%) of annual ET was obtained when all six input variables were included in the analysis.

The p-values for statistics suggest that only the band 5 (B5) and band 7 (B7) variables (0.043 and 3.14E-06) were important in ET remote estimation modeling (tables 4 and 5). When we modeled ET with only these two variables (B5 and B7), an R^2 value of 0.55 and average residual error of 25.46 W m^{-2} (6.18%) were obtained, which was a meager reduction of 0.06 and increase of 0.1%, respectively. This demonstrated that Landsat 7 ETM+ B5 and B7, which are relevant indicators of plant moisture content and soil moisture content (fig. 3), respectively, were also useful parameters in a model of mature pine vegetation ET. The p-value statistics (B5 = 0.051 and B7 = 4.07E-07) also suggest that both input variables were significant in model development for remote estimation of mature pine vegetation ET. This also confirmed that SAVI, NDVI, and CVI input parameters were strongly collinear and did not contribute to model development.

A stepwise regression analysis was completed to ascertain the best contributing model variables. Table 6 contains the results obtained with 40 datasets (with outliers) and 35 datasets (without outliers). The best model obtained through the stepwise analysis was with B5 and B7 as the predictor, with n = 41 (without outliers) and R^2 of 0.48. In addition, with 35 datasets (without outliers), B7 only was shown as the best contributing variable, with R^2 = 0.5.

Table 4a. Regression statistics for six-parameter model.

Multiple R	0.783211629
R^2	0.613420456
Adjusted R^2	0.530581982
Standard error	157.3127591
Observations	35

Therefore, we conclude that B5 and B7 are the most important contributing input variables for remote estimation of homogenous mature pine vegetation ET. Complete results are given in the Appendices at the end of this article.

The model equation obtained from the study is provided in equation 5:

ET of mature homogenous pine vegetation (W m^{-2}) =

$$534.89 + (4.46 \times \text{B5 mean}) - (3.44 \times \text{B7 mean}) \quad (5)$$

The result suggests that the hourly ET (W m^{-2}) for a homogenous pine forest can be estimated efficiently using freely available Landsat imagery. However, the ET prediction model needs further improvement by including additional data from other spatial locations with varying climatic conditions and data of more temporal variation. Studies may also be warranted to examine the capability of the method to estimate ET and its associated parameters for younger pine forests.

CONCLUSIONS

The study suggests that plant canopy temperature, canopy conductance (g_c), and ET for a mature pine forest with a closed canopy can be estimated reasonably well on a spatial basis using the freely available Landsat image-based digital information. The study results suggest that remotely sensed data can be used to estimate mature pine ET without cumbersome and costly direct measurement. Thus, the assessment of hydrologic impacts of site-specific vegetation management on large spatial scales could be conducted using remotely sensed data. Particularly, Landsat band 6 (TIR) showed very high correlation with upper-canopy air temperature, which is one of the critical parameters for estimating ET. Band 5 (MIR) showed low correlation with pine g_c,

Table 4b. ANOVA for six-parameter model.

	df	SS	MS	F	Significance F
Regression	6	1099525.516	183254.3	7.405019	8.17E-05
Residual	28	692924.5172	24747.3		
Total	34	1792450.034			

	Coefficient	Standard Error	t-Statistic	p-Value	Lower 95%	Upper 95%
Intercept	176.3671883	210.4845298	0.83791	0.409177	-254.791	607.5252
Band 5	5.525177404	2.602544714	2.12299	0.042729	0.194106	10.85625
Band 6	0.976680833	0.963592067	1.013583	0.319461	-0.99715	2.95051
Band 7	-3.583705159	0.617840535	-5.80037	3.14E-06	-4.84929	-2.31812
NDVI	1005.417124	1299.409105	0.773749	0.445563	-1656.3	3667.136
SAVI	-193.573593	711.6937162	-0.27199	0.787625	-1651.41	1264.265
CVI	-661.9462176	536.8292275	-1.23307	0.227803	-1761.59	437.6986

Table 5a. Regression statistics for B5 and B7 model.

Multiple R	0.74628
R^2	0.556933
Adjusted R^2	0.529242
Standard error	157.5372
Observations	35

Table 6. Stepwise regression results to determine important input variables for ET estimation model development.

Model	Input Parameter Combination	R^2	Adjusted R^2
1	B7 (with 40 datasets)	0.31	0.29
2	B5 and B7 (with 40 datasets)	0.48	0.45
3	B7 (with 35 datasets)	0.50	0.49

Table 5b. ANOVA for B5 and B7 model.

	df	SS	MS	F	Significance F	
Regression	2	998274.9	499137.5	20.11193	2.21E-06	
Residual	32	794175.1	24817.97			
Total	34	1792450				
	Coefficient	Standard Error	t-Statistic	p-Value	Lower 95%	Upper 95%
Intercept	534.8906	111.1649	4.811684	3.43E-05	308.455	761.3262
Band 5	4.458386	2.202602	2.024145	0.051371	-0.02817	8.94494
Band 7	-3.43791	0.54225	-6.34008	4.07E-07	-4.54244	-2.33338

although additional data and further study are warranted before this relationship is discounted. The need remains to develop a more significant, robust algorithm for predicting mature pine g_c, which is a critical biological variable in physically based ET models such as Penman-Monteith (Amatya et al., 1996). Band 7 (MIR) was not correlated with soil moisture content in the pine forest, likely because the closed pine canopy, understory, and/or forest litter ground cover created obstacles for sensing the soil characteristics remotely. Bands 5 and 7 of the Landsat 7 ETM+ digital information correlated well with the homogenous mature pine ET values in this study. New studies are underway to model soil moisture status in young pine plantations, where canopy cover is thin and between-row bare soil is visible.

In the future, better data mining (data gap filling, outlier exclusion, data exclusion with better understanding of microclimate in the field, etc.) needs to be conducted for robust ET and ET-parameter model development, accounting for the uncertainty of both data and models. Inclusion of spatial variability with eddy flux tower-based forest ET data from multiple locations should be part of the model development process to develop robust models for various forest types and stand ages. Furthermore, methods to extrapolate ET that has been estimated intermittently using a remote sensing approach to seasonal and annual scales should be developed and tested with ground-truth data, as was recently shown by Cammalleri et al. (2013) using a data-fusion approach with high-resolution, low-frequency Landsat imagery and low-resolution, high-frequency MODIS data. Finally, there is a need for further research to develop a soil moisture model for dense canopy pine forest cover with high-resolution imagery and localized *in situ* soil moisture measurements.

ACKNOWLEDGEMENTS

The authors would like to acknowledge Dr. Asko Noormets of the USDA Forest Service for timely help with the field data and astute suggestions in the research development. Similarly, the authors would like to thank Dr. Jami Nettles and Cliff Tyson of Weyerhaeuser Company for their logistics support of this study.

REFERENCES

Amatya, D. M. (1993). Hydrologic modeling of drained forested lands. PhD diss. Raleigh, NC: North Carolina State University.

Amatya, D. M., & Skaggs, R. W. (2001). Hydrologic modeling of pine plantations on poorly drained soils. *Forest Sci., 47*(1), 103-114.

Amatya, D. M., Harrison, C. A., & Trettin, C. C. (2014). Comparison of potential evapotranspiration (PET) using three methods for a grass reference and a natural forest in coastal plain of South Carolina. In *Proc. 2014 South Carolina Water Resour. Conf.* Clemson, SC: Clemson University.

Amatya, D. M., Skaggs, R. W., & Gregory, J. D. (1996). Effects of controlled drainage on the hydrology of drained pine plantations in the North Carolina coastal plain. *J. Hydrol., 181*(1-4), 211-232. http://dx.doi.org/10.1016/0022-1694(95)02905-2

Ambrose, A. R., Sillett, S. C., Koch, G. W., Van Pelt, R., Antoine, M. E., & Dawson, T. E. (2010). Effects of height on treetop transpiration and stomatal conductance in coast redwood (*Sequoia sempervirens*). *Tree Physiol., 30*(10), 1260-1272. http://dx.doi.org/10.1093/treephys/tpq064

Anderson, M. C., Neale, C. M. U., Li, F., Norman, J. M., Kustas, W. P., Jayanthi, H., & Chavez, J. (2004). Upscaling ground observations of vegetation water content, canopy height, and leaf area index during SMEX02 using aircraft and Landsat imagery. *Remote Sens. Environ., 92*(4), 447-464. http://dx.doi.org/10.1016/j.rse.2004.03.019

Bastiaanssen, W. G. M., Menenti, M., Feddes, R. A., & Holtslag, A. A. M. (1998). A remote sensing surface energy balance algorithm for land (SEBAL): 1. Formulation. *J. Hydrol., 212-213*, 198-212. http://dx.doi.org/10.1016/S0022-1694(98)00253-4

Brauman, K. A., Freyberg, D. L., & Daily, G. C. (2012). Potential evapotranspiration from forest and pasture in the tropics: A case study in Kona, Hawaii. *J. Hydrol., 440-441*, 52-61. http://dx.doi.org/10.1016/j.jhydrol.2012.03.014

Cammalleri, C., Anderson, M. C., Gao, F., Hain, C. R., & Kustas, W. P. (2013). A data fusion approach for mapping daily evapotranspiration at field scale. *Water Resour. Res., 49*(8), 4672-4686. http://dx.doi.org/10.1002/wrcr.20349

Carter, G. A. (1998). Reflectance wavebands and indices for remote estimation of photosynthesis and stomatal conductance in pine canopies. *Remote Sens. Environ., 63*(1), 61-72. http://dx.doi.org/10.1016/S0034-4257(97)00110-7

Chen, J. M., Rich, P. M., Gower, S. T., Norman, J. M., & Plummer, S. (1997). Leaf area index of boreal forests: Theory, techniques, and measurements. *J. Geophys. Res. Atmos., 102(D24)*, 29,429-29,443. http://dx.doi.org/10.1029/97JD01107

Colombo, R., Bellingeri, D., Fasolini, D., & Marino, C. M. (2003). Retrieval of leaf area index in different vegetation types using high-resolution satellite data. *Remote Sens. Environ., 86*(1), 120-131. http://dx.doi.org/10.1016/S0034-4257(03)00094-4

Curran, P. (1980). Multispectral remote sensing of vegetation amount. *Prog. Phys. Geog., 4*(3), 315-341. http://dx.doi.org/10.1177/030913338000400301

Gamon, J. A., Field, C. B., Goulden, M. L., Griffin, K. L., Hartley, A. E., Joel, G., ... Valentini, R. (1995). Relationships between NDVI, canopy structure, and photosynthesis in three Californian vegetation types. *Ecol. Appl., 5*(1), 28-41. http://dx.doi.org/10.2307/1942049

Hafeez, M. M., Chemin, Y., & Geisen, V. D., & Bouman, B. A. M. (2002). Field evapotranspiration estimation in central Luzon, Philippines, using different sensors: LandSat 7ETM+, Terra Modis, and Aster. In *Proc. Symp. on Geospatial Theory, Processing, and Applications.* Intl. Society for Photogrammetry and Remote Sensing (ISPRS).

Hilker, T., Hall, F. G., Coops, N. C., Collatz, J. G., Black, T. A., Tucker, C. J., ... Grant, N. (2013). Remote sensing of transpiration and heat fluxes using multi-angle observations. *Remote Sens. Environ., 137*, 31-42. http://dx.doi.org/10.1016/j.rse.2013.05.023

Huete, A. R. (1988). A soil-adjusted vegetation index (SAVI). *Remote Sens. Environ., 25*(3), 295-309. http://dx.doi.org/10.1016/0034-4257(88)90106-X

Hwang, T., Band, L., & Hales, T. C. (2009). Ecosystem processes at the watershed scale: Extending optimality theory from plot to catchment. *Water Resour. Res., 45*(11), W11425. http://dx.doi.org/10.1029/2009WR007775

Jensen, M. E., Burman, R. D., & Allen, R. G. (1990). Evapotranspiration and irrigation water requirements. Manuals and Reports on Eng. Practice No. 70. Reston, VA: ASCE.

Justice, C. O., Vermote, E., Townshend, J. R. G., Defries, R., Roy, D. P., Hall, D. K., ... Barnsley, M. J. (1998). The moderate resolution imaging spectroradiometer (MODIS): Land remote sensing for global change research. *IEEE Trans. Geosci. Remote Sens., 36*(4), 1228-1249. http://dx.doi.org/10.1109/36.701075

le Maire, G., François, C., Soudani, K., Davi, H., Le Dantec, V., Saugier, B., & Dufrěne, E. (2006). Forest leaf area index determination: A multiyear satellite-independent method based on within-stand normalized difference vegetation index spatial variability. *J. Geophys. Res. Biogeosci., 111*(G2), G02027. http://dx.doi.org/10.1029/2005JG000122

Lee, J. G. (1994). Counterspace operations for information dominance. Maxwell AFB, AL: Air University, School of Advanced Airpower Studies.

Lillesand, T. M., & Kiefer, R. W. (1994). *Remote sensing and image interpretation* (3rd ed.). New York, NY: John Wiley and Sons.

Malone, R. W., Yagow, G., Baffaut, C., Gitau, M., Qi, Z., Amatya, D. M., ... Green, T. (2014). Parameterization guidelines and considerations for hydrologic models. *Trans. ASABE, 58*(6), 1681-1703. http://dx.doi.org/10.13031/trans.58.10709

McCarthy, E. J., Skaggs, R. W., & Famum, P. (1991). Experimental determination of the hydrologic components of a drained forest watershed. *Trans. ASAE, 34*(5), 2031-2039. http://dx.doi.org/10.13031/2013.31833

Moran, M. S., Clarke, T. R., Inoue, Y., & Vidal, A. (1994). Estimating crop water deficit using the relation between surface-air temperature and spectral vegetation index. *Remote Sens. Environ., 49*(3), 246-263. http://dx.doi.org/10.1016/0034-4257(94)90020-5

Morris, J., Mann, L., & Collopy, J. (1998). Transpiration and canopy conductance in a eucalypt plantation using shallow saline groundwater. *Tree Physiol., 18*(8-9), 547-555. http://dx.doi.org/10.1093/treephys/18.8-9.547

Narasimhan, B., Srinivasan, R., & Whittaker, A. D. (2003). Estimation of potential evapotranspiration from NOAA-AVHRR satellite. *Appl. Eng. Agric., 19*(3), 309-318. http://dx.doi.org/10.13031/2013.13667

Nghi, V. V., Dung, D. D., & Lam, D. T. (2008). Potential evapotranspiration estimation and its effect on hydrological model response at the Nong Son basin. *VNU J. Sci., Earth Sci., 24*(2008), 213-223.

Noormets, A., Gavazzi, M. J., McNulty, S. G., Domec, J.-C., Sun, G. E., King, J. S., & Chen, J. (2010). Response of carbon fluxes to drought in a coastal plain loblolly pine forest. *Global Change Biol., 16*(1), 272-287. http://dx.doi.org/10.1111/j.1365-2486.2009.01928.x

North, P. R. J. (2002). Estimation of fAPAR, LAI, and vegetation fractional cover from ATSR-2 imagery. *Remote Sens. Environ., 80*(1), 114-121. http://dx.doi.org/10.1016/S0034-4257(01)00292-9

Nouri, H., Beecham, S., Kazemi, F., & Hassanli, A. M. (2013). A review of ET measurement techniques for estimating the water requirements of urban landscape vegetation. *Urban Water J., 10*(4), 247-259.

Olioso, A., Chauki, H., Courault, D., & Wigneron, J.-P. (1999). Estimation of evapotranspiration and photosynthesis by assimilation of remote sensing data into SVAT models. *Remote Sens. Environ., 68*(3), 341-356. http://dx.doi.org/10.1016/S0034-4257(98)00121-7

Oren, R., Sperry, J. S., Katul, G. G., Pataki, D. E., Ewers, B. E., Phillips, N., & Schafer, K. V. R. (1999). Survey and synthesis of intra- and interspecific variation in stomatal sensitivity to vapour pressure deficit. *Plant Cell Environ., 22*(12), 1515-1526. http://dx.doi.org/10.1046/j.1365-3040.1999.00513.x

Panda, S. S., Amatya, D. M., & Hoogenboom, G. (2014). Stomatal conductance, canopy temperature, and leaf area index estimation using remote sensing and OBIA techniques. *J. Spatial Hydrol., 12*(1).

Panda, S. S., Peters, P., Harris, R., & Skarda, R. J. (2011). Remote measurement of potential water loss through evapotranspiration of kudzu during the growing season. Poster presented at the 2001 National Water Conference (Jan. 31 to Feb. 1, 2011, Washington, DC).

Panda, S. S., Rao, M. N., Fitzerald, J. E., & Thenkabail, P. S. (2015). Remote sensing system-platforms and sensors: Aerial, satellite, UAV, optical, radar, and LiDAR. In P. Thenkabail (Ed.), *Remote sensing handbook*, Vol. 1. Boca Raton, FL: CRC Press.

Pearcy, R. W., Schulze, E. D., & Zimmermann, R. (1989). Measurement of transpiration and leaf conductance. In *Plant physiological ecology* (pp. 137-160). New York, NY: Springer Science.

Provoost, S., Van Til, M., Deronde, B., & Knotters, A. (2005). Remote sensing of coastal vegetation in the Netherlands and Belgium. In *Proc. Dunes and Estuaries 2005: Intl. Conf. Nature Restoration Practices in European Coastal Habitats* (pp. 139-149). VLIZ Special Publication 19. Ostend, Belgium: Flanders Marine Institute.

Qi, J., Kerr, Y. H., Moran, M. S., Weltz, M., Huete, A. R., Sorooshian, S., & Bryant, R. (2000). Leaf area index estimates using remotely sensed data and BRDF models in a semiarid region. *Remote Sens. Environ., 73*(1), 18-30. http://dx.doi.org/10.1016/S0034-4257(99)00113-3

Rao, N. R., Garg, P. K., & Ghosh, S. K. (2006). Estimation and comparison of leaf area index of agricultural crops using 1248 IRS LISS-III and 1249 EO-1 hyperion images. *J. Indian Soc. Remote Sens., 34*(1), 69-78. http://dx.doi.org/10.1007/bf02990748

Rouse, J. W., Haas, R. H., Schell, J. A., & Deering, D. W. (1973). Monitoring vegetation systems in the Great Plains with ERTS. In *Proc. 3rd ERTS Symp.* (pp. 309-317). NASA SP-351. Greenbelt, MD: NASA Goddard Spaceflight Center.

Sack, L., & Scoffoni, C. (2012). Measurement of leaf hydraulic conductance and stomatal conductance and their responses to irradiance and dehydration using the evaporative flux method

(EFM). *J. Visualized Experience (JoVE)*, 70, e4179. http://dx.doi.org/10.3791/4179

Sampson, D. A., Amatya, D. M., Blanton Lawson, C. D., & Skaggs, R. W. (2011). Leaf area index (LAI) of loblolly pine and emergent vegetation following a harvest. *Trans. ASABE, 54*(6), 2057-2066. http://dx.doi.org/10.13031/2013.40664

Senay, G. B., Bohms, S., Singh, R. K., Gowda, P. H., Velpuri, N. M., Alemu, H., & Verdin, J. P. (2013). Operational evapotranspiration mapping using remote sensing and weather datasets: A new parameterization for the SSEB approach. *JAWRA, 49*(3) 577-591. http://dx.doi.org/10.1111/jawr.12057

Shuttleworth, W. J. (2008). Evapotranspiration measurement methods. *Southwest Hydrol., 7*(1), 22-23.

Soudani, K., François, C., le Maire, G., Le Dantec, V., & Dufrĕne, E. (2006). Comparative analysis of IKONOS, SPOT, and ETM+ data for leaf area index estimation in temperate coniferous and deciduous forest stands. *Remote Sens. Environ., 102*(1-2), 161-175. http://dx.doi.org/10.1016/j.rse.2006.02.004

Sun, G., Alstad, K., Chen, J., Chen, S., Ford, C. R., Lin, G., ... Zhang, Z. (2011). A general predictive model for estimating monthly ecosystem evapotranspiration. *Ecohydrology, 4*(2), 245-255. http://dx.doi.org/10.1002/eco.194

Sun, G., Noormets, A., Gavazzi, M. J., McNulty, S. G., Chen, J., Domec, J. C., ... Skaggs, R. W. (2010). Energy and water balance of two contrasting loblolly pine plantations on the lower coastal plain of North Carolina. *Forest Ecol. Mgmt., 259*(7), 1299-1310. http://dx.doi.org/10.1016/j.foreco.2009.09.016

Tian, S., Youssef, M. A., Skaggs, R. W., Amatya, D. M., & Chescheir, G. M. (2012). DRAINMOD-Forest: Integrated modeling of hydrology, soil carbon and nitrogen dynamics, and plant growth for drained forests. *J. Environ. Qual., 41*(3), 764-782. http://dx.doi.org/10.2134/jeq2011.0388

Turner, D. P., Cohen, W. B., Kennedy, R. E., Fassnacht, K. S., & Briggs, J. M. (1999). Relationships between leaf area index and Landsat TM spectral vegetation indices across three temperate zone sites. *Remote Sens. Environ., 70*(1), 52-68. http://dx.doi.org/10.1016/S0034-4257(99)00057-7

USDA. (2014). Database for landscape-scale carbon monitoring sites. Newtown Square, PA: USDA Forest Service, Northern Research Station. Retrieved from http://www.nrs.fs.fed.us/data/lcms/tpt/

Viessman, W., & Lewis, G. L. (2004). *Introduction to Hydrology.* Upper Saddle River, NJ: Prentice Hall.

Wang, L., & Qu, J. J. (2009). Satellite remote sensing applications for surface soil moisture monitoring: A review. *Front. Earth Sci. China, 3*(2), 237-247. http://dx.doi.org/10.1007/s11707-009-0023-7

Wang, Q., Adiku, S., Tenhunen, J., & Granier, A. (2005). On the relationship of NDVI with leaf area index in a deciduous forest site. *Remote Sens. Environ., 94*(2), 244-255. http://dx.doi.org/10.1016/j.rse.2004.10.006

Wilson, K. B., Hanson, P. J., Mulholland, P. J., Baldocchi, D. D., & Wullschleger, S. D. (2001). A comparison of methods for determining forest evapotranspiration and its components: Sap-flow, soil water budget, eddy covariance, and catchment water balance. *Agric. Forest Meteorol., 106*(2), 153-168. http://dx.doi.org/10.1016/S0168-1923(00)00199-4